D. Fritsch, M. Englich & M. Sester, eds, 'IAPRS', Vol. 32/4, ISPRS Commission IV Symposium on GIS - Between Visions and Applications, Stuttgart, Germany.

PHOTOGRAMMETRIC POINT DETERMINATION AND DEM GENERATION USING MOMS-2P/PRIRODA THREE-LINE IMAGERY

Wolfgang Kornus, Manfred Lehner
German Aerospace Center (DLR), Institute of Optoelectronics, Optical Remote Sensing Division,D-82230 Wessling, Germany
e-mail: Wolfgang.Kornus@dlr.de, Manfred.Lehner@dlr.de

Heinrich Ebner, Harald Fröba,* Timm Ohlhof*
Technical University Munich, Chair for Photogrammetry and Remote Sensing,D-80290 Munich, Germany
e-mail: ebn@photo.verm.tu-muenchen.de, hfroeba@esg-gmbh.de, tohlhof@esg-gmbh.de

Commission IV, Working Group IV/4

KEY WORDS: MOMS-2P, Three-Line Imagery, Self Calibration, Bundle Adjustment, Point Determination, DEM Generation, Accuracy

ABSTRACT

This paper describes the process of photogrammetric point determination by bundle adjustment using three-line imagery collected by MOMS-2P, the German **M**odular **O**ptoelectronic **M**ultispectral **S**canner. Since May 1996 MOMS-2P is attached to the remote sensing module PRIRODA of the Russian space station MIR. Its stereo module with three differently oriented lenses allows for the acquisition of three-fold along track stereoscopic imagery. The forward and aft looking channels provide 18 m, the nadir looking high resolution (HR) channel 6 m ground pixel size. For the photogrammetric evaluation 9 image scenes of orbit T083C were composed to an approximately 415 km long image strip covering parts of Southern Germany and Austria. For the German part control points provided by AMilGeo (Amt für Militärisches Geowesen) were used as ground control, with an accuracy of 1.5 m in X, Y and Z. The navigation data are recorded simultaneously with the image lines by the MOMS-NAV package mounted next to MOMS-2P on the PRIRODA module. The orbit positions are expected to have 5 m absolute and 3 m relative accuracy. The INS data have a relative accuracy of $15''$. Since MOMS was mounted in orbit during an extra vehicular activity (EVA), there is no precise absolute pointing knowledge of the MOMS camera axes. According to experiences of earlier MOMS data evaluations the camera geometry is simultaneously estimated by self calibration methods. Using small subsets of 12, 7 and 4 control points empirical accuracies of approximately 8 m in planimetry and 10 m in height are achieved, verified by 141 independent check points. Finally a digital elevation model is produced for the entire area (about 50 km $\times$ 100 km), which is imaged by all three stereo channels. For that purpose about 700.000 points are transformed into object space using the estimated interior and exterior orientation of the bundle adjustment. The comparison with a reference digital terrain model of AMilGeo results in normally distributed height differences with a standard deviation also of 10 m, demonstrating that the achieved accuracy of point determination is valid for the entire area.

1 INTRODUCTION

During the MOMS-2P/PRIRODA mission, launched in April 1996, the Modular Optoelectronic Multispectral Scanner MOMS-2P acquires digital high resolution, along track, threefold stereoscopic and multispectral imagery of the Earth's surface from the Russian space station MIR. The MOMS-2P/PRIRODA mission was the second use of MOMS in space after the successful MOMS-02/D2 experiment in 1993.

The photogrammetric processing of the MOMS-2P/PRIRODA data is conducted by several German university institutes and DLR's Institute of Optoelectronics. The major aim is to realize the entire photogrammetric processing chain, which starts with radiometrically corrected image data and ends up with digital elevation models (DEM), orthoimage maps and vector data for geo-information-systems (GIS). Within the science team the Chair for Photogrammetry and Remote Sensing of the Technical Univerity Munich is responsible for the reconstruction of the exterior orientation by combined adjustment and the semi-automatic extraction of linear objects for updating the German GIS ATKIS-DLM25.

The main parameters of the MOMS-2P/PRIRODA mission compared to the MOMS-02/D2 experiment are listed in Table 1. In contrast to the D2 mission, the MIR orbital inclination of 51.6° also allows for imaging of industrial countries in Europe and North America. Due to several problems, only a few MOMS-2P/PRIRODA data takes were acquired between September 1996 and April 1997. Since January 1998 MOMS-2P is again operating.

The optical system of MOMS-02 consists of a stereo module and a multispectral module, where in 4 different imaging modes certain combinations of the panchromatic stereo and the multispectral channels can be selected. The 3 lenses of the stereo module provide 3-fold along track stereo scanning with different ground resolutions. The nadir looking HR channel (6 m ground pixel size) comprises 2 arrays with 6000 sensor elements each, which are optically combined to 1 array with 9000 sensor elements. The other CCD arrays consist of 6000 sensor elements (18 m ground pixel size). In stereo imaging mode A 8304 sensor elements of the HR channel and 2976 sensor elements of the stereo channels are active. More details can be found in (Seige et al., 1998).

	MOMS-02/D2	**MOMS-2P/PRIRODA**
Camera carrier:	Space shuttle	MIR space station
Mission duration:	10 days	at least 18 months
Orbital height:	296 km	400 km
Orbital inclination:	28.5°	51.6°
Ground pixel [m]:	4.5 (HR) / 13.5	6.0 (HR) / 18.0
Swath (mode A):	37 km	50 km
Orbit information:	TDRSS tracking	GPS
Attitude information:	Shuttle-IMU	MOMS-IMU, star sensor

Table 1: Parameters of MOMS-02/D2 and MOMS-2P/PRIRODA

On March 14th, 1997, the first MOMS-2P imagery of Germany in stereo imaging mode A was taken. For the photogrammetric evaluation 9 image scenes of orbit T083C were composed to an approximately 415 km long image strip covering parts of Southern Germany and Austria. In the following section the initial information for the combined point determination like imagery, calibration data, image coordinates of tie points, navigation and ground control information is described. After a short review of the functional model and a summary of the input data the results of the combined bundle adjustment are presented and assessed. Additionally a DEM with 50 m grid size is generated and compared to a 5 m accurate

*now: Elektroniksystem- und Logistik-GmbH (ESG), D-81605 Munich

D. Fritsch, M. Englich & M. Sester, eds, 'IAPRS', Vol. 32/4, ISPRS Commission IV Symposium on GIS - Between Visions and Applications, Stuttgart, Germany.

reference DEM. Finally the experiences are summarized and conclusions are drawn.

2 INITIAL DATA

2.1 Image data

Due to high cloud coverage in the western part of the strip, the evaluation starts with image scene #25, approximately at the longitude of Stuttgart (see Figure 1). The end of the strip has been selected about 160 km beyond the Austrian border in image scene #33. Thus, the control and check points, which all are located in Germany (see section 2.5) are also imaged by the backward looking channel ST7. The ground pixel size of the imagery is 5.9 m and 17.7 m at 390 km orbit height. The image quality of the HR channel is adversely affected (strong defocussing effects), due to technical problems, which occured during the warming-up phase of the scanner and are documented in the temperature measurements of the housekeeping data.

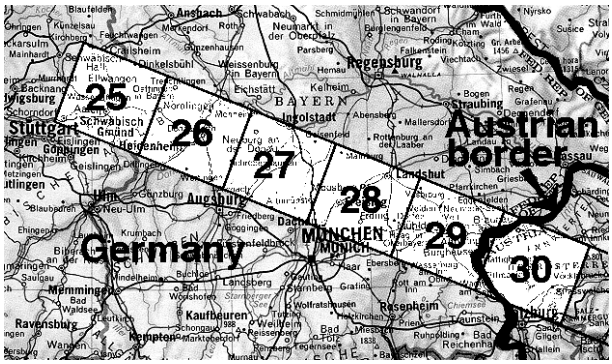

Figure 1: Geographic location of the test area

2.2 Calibration data

The geometric system calibration has been conducted at the laboratories of the German aerospace company Dasa, where MOMS has been developed and manufactured. A summarizing description of the procedure is given in (Kornus et al., 1996). From the calibration measurements a refined camera model has been developed, rigorously modelling the geometry of each CCD-array by 5 parameters:

- 2 displacements x_0, y_0 and
- 1 rotation of the CCD-array in the image plane κ,
- 1 deviation of the focal length dc and
- 1 parameter K modelling the sensor curvature.

The model and the derivation of model parameters from the calibration measurements are comprehensively described in (Kornus, 1996a), (Kornus, 1997b). The photogrammetric evaluation of MOMS-02/D2 imagery led to the assumption, that in orbit significant deviations of the camera geometry from the lab-calibration results appeared (Kornus et al., 1995), (Lehner and Kornus, 1996), (Kornus, 1997b), which later were confirmed by evaluation of MOMS-2P/PRIRODA imagery, first for the nadir viewing (multispectral and HR) channels in the course of band to band registration (Lehner, 1996), (Kornus, 1996b), (Lehner and Kornus, 1997) and also for the stereo channels in the course of photogrammetric point determination using accurate ground control (Kornus and Lehner, 1997), (Kornus et al., 1998).

The camera parameters in Table 2 are taken from (Kornus, 1996a) and (Kornus, 1997a). They basically reflect the status of laboratory calibration already considering the relative displacement of channel 5B (with respect to 5A), which was detected by matching 5A- and 5B-imagery within the (nominal) 10 pixel wide overlap (Lehner, 1997). All parameters are fed into the bundle adjustment with low weights allowing for selfcalibration, i. e. possible changes of the parameter values p in the order of the a priori standard deviation σ_p are considered and simultaneously estimated in the bundle adjustment.

	HR5A (reference)		HR5B	
	p	σ_p	p	σ_p
c [mm]	660.256	0.050	660.224	0.050
x_0 [pixel]	0.1	—	0.2	3.0
y_0 [pixel]	-0.4	—	0.1	3.0
K [pixel]	-0.3	1.0	-0.4	1.0
κ [mdeg]	-2.9	—	5.4	10.0
	ST6		ST7	
	p	σ_p	p	σ_p
c [mm]	237.241	0.050	237.246	0.050
x_0 [pixel]	-7.2	3.0	-0.5	3.0
y_0 [pixel]	8.0	3.0	19.2	3.0
K [pixel]	-1.1	1.0	1.7	1.0
κ [mdeg]	-1.5	10.0	-1.4	10.0

Table 2: Lab-calibrated camera parameters p and their a priori standard deviations σ_p

The sensor curvature is modeled by a second order polynomial. The parameter K here indicates the along track deviation at the edges of the CCD-array at 3000 pixel distance from the array center, which is caused by the sensor curvature.

2.3 Image coordinates of tie points

DLR matching software has been used to derive image coordinates of tie points. This software aims at the automated measurement of massive numbers of tie points in the stereoscopic imagery of 3-line stereo scanners like MOMS. The matching is purely done in image space as it is meant to provide tie points for photogrammetric adjustment of stereo imagery from various sources. If available, it will exploit the presence of 3 stereo pairs for further effective blunder reduction. The data flow of this matching concept is shown in Figure 2.

Its main features are:

1. An interest operator selects well defined patterns suitable for digital image correlation; the principles of the Förstner interest operator are used with slight modification; a good interest operator point is defined by a surrounding window with multidirectional edge information and a local contrast above a given threshold; pattern sizes of 7 x 7 pixels (4 lower resolution levels of the image pyramid) and 9 x 9 pixels (2 high resolution levels of the image pyramid) have been used for this data set; the threshold for the Förstner parameter roundness has been set to 0.85, the grey value variance of the patterns was not allowed to drop below 25.
2. Conjugate points on pixel accuracy level are generated using the maximum of the normalized correlation coefficient; the latter and a quality figure describing the steepness and uniqueness of the peak in the matrix of correlation coefficients are stored for later subselection of tie points; the positioning of the search areas is done via an affine transformation which is calculated using already known tie points in the neighbourhood (normally, an image pyramid is used for getting these approximate points); for T083C search area sizes of 15 x 15 up to 27 x 27 pixels have been used for the 6 levels of the image pyramid to cope with the increase of parallaxes at the higher levels of the pyramid; the mean of the maximum of correlation

D. Fritsch, M. Englich & M. Sester, eds, 'IAPRS', Vol. 32/4, ISPRS Commission IV Symposium on GIS - Between Visions and Applications, Stuttgart, Germany.

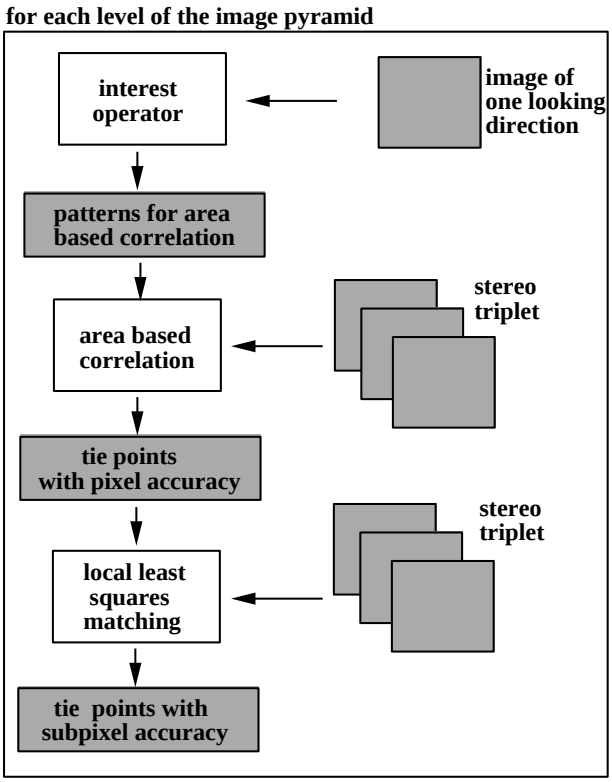

Figure 2: data flow diagram of matching in image space

coefficients for T083C is about 0.9 which illustrates the good matching potential of along-track stereo imagery.

3. Local least squares matching (LLSQM) is finally used for refinement of the image coordinates of the tie points to subpixel accuracy; in this step it is also possible to match images of different resolution like MOMS high and low resolution channels; this multi-scale feature is used here for the completion of manual measurements to full tie points (good initial approximations can be generated via local affine transformation calculated by using the massive number of tie points found at this matching stage, see 2.5.1); the mean number of iterations for the iterative adjustment of 6 geometric and 2 radiometric parameters in LLSQM lies normally between 3 and 4.

4. All steps are performed for each level of an image pyramid in order to make the process more robust by progressing from coarse to fine resolution, i.e. from small parallaxes to larger ones; an image pyramid of 6 resolution levels has been used for T083C.

More details on the matching software can be found in (Lehner, 1986), (Lehner and Gill, 1992), (Lehner and Kornus, 1996), and (Kornus et al., 1996). About 350,000 tie points have been found. For these a standard deviation of 0.2 pixel for both image coordinates has been introduced into the adjustment. Even if the potential of LLSQM is about 0.1 pixel, this is not achievable but for neat patterns not containing parts of complex objects like trees and houses.

2.4 Navigation data

MOMS-2P has its own navigation system MOMS-NAV consisting of a Motorola Viceroy GPS receiver with dual antennas and LITEF gyro systems. The raw GPS and gyro data are recorded along with the MOMS image frames. Additionally, information for later exact synchronization of MOMS-NAV data generation timings and image frame numbers is written into these auxiliary housekeeping data. This synchronization is done via two electronic counters. From the values of these counters the time delay between navigation data generation and first writing into frameheader can be calculated.

MOMS-NAV allows for up to now unprecedented accuracies of orbit and attitude for an imaging device in space.

2.4.1 Attitude data The processing of the gyro data including the absolute referencing with INS data of the Mir station or - if available - star camera measurements using the star sensor on Mir module Kvant 2 takes place at the German Space Operations Center (GSOC) of DLR. This also includes the time synchronization of navigation data and image frames. The angular and velocity increments provided by the gyro unit at a rate of about 120 Hz are converted into Euler angles in WGS-84 coordinate system for a 2-1-3 Euler angle rotational sequence. For the data take T083C discussed here a standard deviation of the angular measurements of $15.3''$ is indicated, corresponding to about 1.6 pixel (ST-channel). Star camera measurements were available. The star camera is on Mir module Kvant 2 and the MOMS camera was mounted by an extravehicular activity onto module PRIRODA (May 1996). Because it was impossible to conduct exact calibration measurements for MOMS orientation on PRIRODA and because of the uncertainties in the overall arrangement of the modules of the Mir station there remains an unknown rotation matrix to be estimated via bundle adjustment.

2.4.2 Orbit data The GeoForschungsZentrum (GFZ) Potsdam analyses the GPS raw data and performs differential GPS computations using the geodetic ground station network and geodetic high-precision orbit models to give the orbit position with an absolute accuracy of better than 5 m and a relative accuracy of 3 m (Föckersperger et al., 1997). When computing independently overlapping arcs for T083C GFZ got rms values for the differences in the overlap region of 1.8 m for x, 1.1 m for y and 2.3 m for z. This indicates that the goal of 5 m for the absolute accuracy of the orbital positions was well reached. They are given in WGS-84 coordinate system.

Already in advance of this, GSOC computes orbit positions from the onboard processed GPS data which are downlinked with the low-bitrate telemetry frames. These relatively inaccurate positions can be interpolated with high-precision orbit models to give an absolute accuracy of about 50 m (Gill, 1997). GFZ also computes rms values of the differences between its orbit calculations and GSOC calculations. For T083C rms values of 34.2 m for x, 20.3 m for y and 26.9 m for z have been found which is well within the accuracy specifications of GSOC.

2.5 Ground control and check points

For the German part of the strip topographic maps of scale 1:50000 were provided by AMilGeo containing so-called *navigations points* (NP), where most of them could be identified in the MOMS-2P imagery. These NP were used as control and as check points in the bundle adjustment.

2.5.1 Image coordinates The identification of the NP in the imagery was complicated by the defocussed HR imagery. Since the confident measurement of ground control and check points in the imagery is a precondition for proper accuracy assessment, two independent methods were applied:

1. *Monoscopic* measurement of NP in channel HR5 imagery and subsequent automatic point transfer into stereo channel ST6- and ST7-imagery.

2. *Stereoscopic* measurement of NP in all channel combinations (fore-nadir, nadir-aft, fore-aft) and subsequent averaging of the results.

D. Fritsch, M. Englich & M. Sester, eds, 'IAPRS', Vol. 32/4, ISPRS Commission IV Symposium on GIS - Between Visions and Applications, Stuttgart, Germany.

Three monoscopic data sets were measured by three different operators using two different visualisation software packages, both allowing for sub-pixel measurement accuracy. Table 3 contains the standard deviations σ_x, σ_y and the systematic deviations v_x, v_y as result of their analysis.

HR5				
data set	σ_x [pixel]	σ_y [pixel]	v_x [pixel]	v_y [pixel]
1–2	0.2	0.2	0.2	0.1
1–3	0.3	0.3	0.5	0.4
2–3	0.3	0.2	0.4	0.4

Table 3: Analysis of the monoscopic measurements

Data set 3, which was measured with an alternative software package was rejected after showing systematic effects to data sets 1 and 2 in the order of 0.5 pixel (see Table 3), while the first two data sets show good correspondance. For the further evaluation data set 1 was selected, since it contains more so-called *3-ray-points*, i.e. points in the central 3-ray-area (image scenes #28 (second half) and #29), which is imaged in all 3 viewing directions. Data set 1 contains 170 3-ray- and 110 2-ray-points. In the following it is called **set A**.

In a further step, the same 170 3-ray-points were measured stereoscopally on a Zeiss PHODIS-ST10 digital stereo plotter. Previously the HR imagery was resampled by factor 3 in order to adapt the image scale to the stereo channels. Each point was measured in all three combinations, i.e. the image coordinates were obtained twice in each channel and averaged. From their differences standard deviations were calculated, which are listed in Table 4. In the following the stereoscopic data set is named as **set B**.

channel	σ_x [pixel]	σ_y [pixel]
HR5 (2)–HR5 (1)	0.1	0.2
ST6 (2)–ST6 (1)	0.2	0.2
ST7 (2)–ST7 (1)	0.2	0.2

Table 4: Analysis of the stereoscopic measurements

The standard deviations derived from the coordinate differences of set A and set B are listed in Table 5. The results show no deviations between the two measurement procedures. ¿From the analysis an a priori standard deviation of all measured image coordinates of 0.2 pixel was deduced.

Channel	σ_x [pixel]	σ_y [pixel]
HR5 (stereo)–HR5 (mono)	0.1	0.1
ST6 (stereo)–ST6 (mono)	0.1	0.1
ST7 (stereo)–ST7 (mono)	0.1	0.2

Table 5: Comparison between stereoscopic and monoscopic measurements

2.5.2 Object coordinates Since the navigation data were related to the geocentric WGS-84 coordinate system the object coordinates of the ground control points (GCP) and check points were needed in the same system (X,Y,Z). The coordinates of the NP, however, were given as planimetric UTM coordinates (E,N) in the ED50 system, and the heights H were related to the mean sea level NN. The standard deviations of the E, N and H coordinates amount to 1.5 m.

For the transformation of the E,N,H into X,Y,Z coordinates the following steps were required:

1. Transformation of the E,N coordinates from ED50 to WGS-84 (datum transformation)
2. Transformation of the NN-heights H into ellipsoidal heights h with respect to WGS-84 using given geoidundulations N by h = H + N
3. Transformation of the E,N coordinates into ellipsoidal coordinates φ (latitude) and λ (longitude)
4. Transformation of the φ, λ, h coordinates into X,Y,Z coordinates

The final standard deviations of the NP coordinates were roughly estimated to 2.5 m in X, Y and Z, corresponding to better than 1/2 ground pixel of the HR channel.

3 COMBINED POINT DETERMINATION

3.1 Functional model of the bundle adjustment

The functional model for the reconstruction of the exterior orientation is based on the principle of orientation images, as proposed by (Hofmann et al., 1982). Here the exterior orientation parameters are estimated only at certain time intervalls, while in between the temporal course of the exterior orientation is modeled by a third order polynomial function. The attitude and position information of the navigation data are treated as uncorrelated observations. In this evaluation they are introduced only at the times of the orientation images. Systematic errors in these data like biases and linear drifts are treated as additional unknowns and estimated simultaneously with the other unknowns in the adjustment.

The model of the interior orientation is characterized by a separate image coordinate system for each CCD-array, which is related to the camera fixed coordinate system by a 6 parameter transformation. Together with the focal length c, a twodimensional displacement vector $(x_0, y_0)^T$ of the CCD-array in the respective focal plane and a parameter K modelling the sensor curvature, they form a set of 10 parameters per CCD-array. With this model the geometry of both one-lens- and also multi-lens-cameras like MOMS-2P can rigorously be described. In this evaluation 5 of these 10 parameters per CCD-array are simultaneously estimated in the adjustment (see section 3.3.1) A detailed description of the functional model of the bundle adjustment is given in (Kornus, 1997b).

3.2 Input data

Table 6 gives an overview of all observations and their a priori standard deviations which were fed into the bundle adjustment. For the entire strip 8 orientation images (OI) were employed. The distance between the OI was set to 3330 image lines, corresponding to 8.2 seconds flight time, which proved to be sufficient to model the temporal course of the exterior orientation parameters.

observations		type	a priori σ
2880	tie points	image coord.	0.2 Pixel
280	control points	image coord.	0.2 Pixel
170	control points	image coord.	0.2 Pixel
252	control points	object coord.	6.0 m
8×3	attitude angles	ext. orient.	$15.3''$
8×3	positions	ext. orient.	3 m
3	position biases	ext. orient.	5 m

Table 6: Observations introduced into the bundle adjustment

¿From the 350,000 tie points a subset of the best 2880 points was gridwise selected using the correlation coefficient and the quality figure as selection criterias. The accuracy of the NP coordinates was assumed to be 6 m in X, Y and Z, corresponding to 1 ground pixel of the HR channel. This rather pessimistic value is due to the defocussing effects in the nadir looking channel, which prevented from a more accurate point identification.

The observations of the exterior orientation parameters were introduced only at the times of the orientation images. The bias of the positions was set to 0.0 m with a standard deviation of 5.0 m,

D. Fritsch, M. Englich & M. Sester, eds, 'IAPRS', Vol. 32/4, ISPRS Commission IV Symposium on GIS - Between Visions and Applications, Stuttgart, Germany.

corresponding to the estimated absolute accuracy of orbit determination (see section 2.4). No drift parameters for the positions were considered. For the attitude angles bias and drift parameters were introduced as free unknowns.

3.3 Results

In a first step all ground control points were fed into the bundle adjustment in order to check the consistency of the different data sets. Next, the combined point determination is executed using small subsets of GCP in order to empirically verify the accuracy potential using the remaining points as check points.

3.3.1 Adjustment using all GCP: After a first adjustment run using all control information some tie and ground control points were rejected, if their residuals in the image (and/or object) coordinates exceeded three times the respective standard deviation. The number of rejected and remaining points is listed in Table 7.

	tie points			ground control points		
	3-ray	2-ray	rejected	3-ray	2-ray	rejected
set A	700	2137	43 (1.5%)	156	96	28 (10%)
set B	700	2138	42 (1.5%)	155	–	15 (9%)

Table 7: Final number of tie and ground control points

Table 8 contains the estimated camera parameters $\hat{p}$ and the theoretical standard deviations $\hat{\sigma}_p$ as result of the bundle adjustment for set A. The columns Δp reflect the deviations from the lab-calibrated results in Table 2. Significant deviations, i.e. values exceeding three times the estimated standard deviation, are indicated in boldfaced characters. The results demonstrate, that changes of the camera geometry up to 2.5 pixel occurred since the time of lab-calibration. Displacements in the same order of magnitude have already been proved for multispectral CCD-arrays during the process of band to band registration (Lehner and Kornus, 1997).

	HR5A (reference)			HR5B		
	$\hat{p}$	$\hat{\sigma}_p$	Δp	$\hat{p}$	$\hat{\sigma}_p$	Δp
c [mm]	660.198	0.024	-0.058	660.224	0.024	0.000
x_0 [pixel]	0.10	—	—	0.61	0.14	0.41
y_0 [pixel]	-0.40	—	—	-0.09	0.06	-0.19
K [pixel]	-0.38	0.19	-0.07	-0.32	0.22	0.05
κ [mdeg]	-2.92	—	—	4.40	6.57	-1.02
	ST6			ST7		
	$\hat{p}$	$\hat{\sigma}_p$	Δp	$\hat{p}$	$\hat{\sigma}_p$	Δp
c [mm]	**237.180**	**0.008**	**-0.061**	237.234	0.007	-0.012
x_0 [pixel]	**-4.83**	**0.16**	**2.37**	**-1.27**	**0.15**	**1.77**
y_0 [pixel]	**10.55**	**0.73**	**2.55**	18.86	0.71	-0.34
K [pixel]	-1.15	0.41	-0.07	1.42	0.37	-0.25
κ [mdeg]	7.65	4.51	9.12	-10.24	4.76	-8.82

Table 8: Estimated camera parameters $\hat{p}$, standard deviations $\hat{\sigma}_p$ and deviations Δp from lab-calibration results

The residuals of the observed parameters of the exterior orientation, which were introduced at the times of the orientation images, were in the order of 1 σ a priori and did not exceed 3 times that value, confirming the assumed a priori standard deviations of the navigation data. The estimated bias parameters of the positions are small and therefore not significantly determined. The estimated attitude biases also are small values, considering, that MOMS was attached to the PRIRODA module during an extra vehicular activity (EVA) and thus the camera axes could not be precisely adjusted to the MIR coordinate system, where the absolute attitude data of the ASTRO-1 star sensor are referenced to. An attitude bias of 0.1° however is equivalent to a position bias of approximately 700 m, which is a fairly big value. Since some position and attitude parameters are correlated, real attitude biases can reasonably be estimated only if highly accurate absolute positions are available, like in this example. Under this condition the combined photogrammetric bundle adjustment is capable to provide an absolute attitude solution in addition to the selfcalibration of the camera parameters.

Like the attitude biases the drift parameters all are significantly determined and match the nominal drift rates of the gyro systems, which are specified with 1°–4°/h (Eisfeller et al., 1996). The estimated bias and drift parameters and their standard deviations are summarised in Table 9. Significant values again are marked by boldfaced characters.

	$\hat{X}_0$	$\hat{\sigma}$	$\hat{Y}_0$	$\hat{\sigma}$	$\hat{Z}_0$	$\hat{\sigma}$
Bias [m]	0.2	5.5	-0.3	5.5	0.6	5.5
	$\hat{\varphi}$	$\hat{\sigma}$	$\hat{\omega}$	$\hat{\sigma}$	$\hat{\kappa}$	$\hat{\sigma}$
Bias [deg]	**0.073**	**0.003**	**-0.164**	**0.003**	**0.035**	**0.006**
Drift [deg/min]	**0.051**	**0.005**	**-0.065**	**0.005**	**0.053**	**0.007**

Table 9: Estimated bias and drift parameter

Up to now, this is the only suitable MOMS-2P data take in stereo mode A with sufficient ground truth available, thus allowing for a rigorous inflight calibration of both the interior and exterior orientation parameters. In the future, the results need to be checked and verified using ground truth and imagery of different orbits, taken in the stereo imaging modes A and D.

Table 10 contains the root-mean-square (RMS) values μ of the residuals of the GCP object coordinates. For better interpretation the estimated geocentric WGS-84 coordinates (X, Y, Z) were subsequently transformed into planimetric UTM coordinates (**E**asting, **N**orthing) and ellipsoidal **H**eights and checked against the (also transformed) control point coordinates. For all ground control points in the 3-ray-area the obtained mean planimetric accuracy is approximately 6 m and the mean height accuracy 4.7 m. This is in agreement with the assumed identification uncertainty of 6 m (see section 3.2).

		WGS-84			UTM		
	number	μ_X	μ_Y	μ_Z	μ_E	μ_N	μ_H
set A	156	5.5	6.2	5.7	6.3	6.2	4.7
set B	155	4.9	5.9	5.3	5.9	5.5	4.7

Table 10: RMS values of all 3-ray-GCP [m]

3.3.2 Adjustment using subsets of GCP: In the further evaluation only those 148 control points in the 3-ray-area were used, which were identified in both data sets A and B. From them 7 points were selected as GCP while the remaining 141 served as independent check points. 3 different GCP configurations (1,2,3) were distinguished (see Figure 3): For each of them 3 different types (a,b,c) of exterior orientation observations were used:

- **1:** 7 GCP in 3-ray-area and 5 GCP in 2-ray-area
- **2:** 7 GCP in 3-ray-area
- **3:** 4 GCP in 3-ray-area (1,3,5,7)

- **a:** Position and attitude data
- **b:** Positions only, no attitude
- **c:** No navigation data at all

In Table 11 the results for both data sets A and B are presented. The highest height accuracy is achieved, if 12 GCP, i.e. if also GCP in the 2-ray-area are introduced (Case 1a). However, the difference to the results with 7 GCP in the 3-ray-area only (Case 2a) is not such big and 4 GCP (Case 3a) result in an only 8% worse height accuracy compared to Case 1a. For data set B even no difference between Case 2a and 3a is visible, demonstrating that the number of GCP does not so much affect the accuracy of photogrammetric point determination if precise navigation data are available. This fact was the main argument to equip MOMS-2P with the precise navigation system MOMS-NAV in order to ensure accurate object reconstruction even with a small amount of costly GCP.

D. Fritsch, M. Englich & M. Sester, eds, 'IAPRS', Vol. 32/4, ISPRS Commission IV Symposium on GIS - Between Visions and Applications, Stuttgart, Germany.

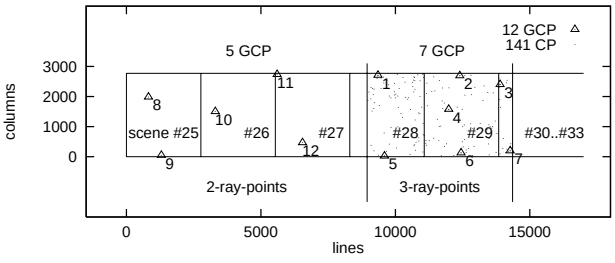

Figure 3: Location of GCP and check points (CP)

The versions b show that the influence of the number of GCP increases, if only orbit information is available, i. e. if the attitude angles are estimated in the photogrammetric adjustment using ground control. 7 GCP are sufficient to establish such stable geometric conditions, that the attitude observations do not improve the results and therefore can be completely neglected (Case 2b). Even if no navigation data are available at all (Case 2c), 7 GCP lead to slightly worse but still comparable accuracies as the Cases 2b and 2a. Here the strength of the along track 3-line stereoscopic images becomes visible, which enable the rigorous reconstruction of spatial objects exclusively by photogrammetric methods and ground control points. This big advantage of 3-line versus 2-line stereoscopy was already found by Dr. Hofmann, the "father" of 3-line-cameras, in the late 70s (Hofmann et al., 1982). However, the results of Case 3 also demonstrate, that navigation data are definitely required if only a small number of GCP is available.

Comparing the results of the two data sets A and B, a tendency can be noticed, that the stereoscopically measured set B leads to higher planimetric accuracies while the monoscopically measured data set A yields better height accuracies. Further runs using only the manually measured control and check points showed, that acceptable accuracies can also be obtained by a small number of tie points, in these examples represented by the check points — 240 in set A and 148 in set B. Thus, large tie point numbers as they are provided by matching processes are not necessarily required for point determination.

	set A						set B					
	WGS-84			UTM			WGS-84			UTM		
Case	ε_X	ε_Y	ε_Z	ε_E	ε_N	ε_H	ε_X	ε_Y	ε_Z	ε_E	ε_N	ε_H
1 a	9.2	8.0	9.5	7.9	8.9	9.8	—	—	—	—	—	—
2 a	7.8	8.2	10.2	8.2	7.9	10.1	8.0	7.6	10.3	7.7	7.2	10.8
2 b	7.7	8.1	10.5	8.2	8.0	10.2	7.9	7.6	10.5	7.7	7.2	10.9
2 c	8.4	8.6	12.5	8.4	9.0	11.2	8.5	8.3	12.0	8.2	7.6	11.1
3 a	7.4	8.6	11.0	8.7	7.9	10.6	7.6	7.9	10.3	7.8	7.0	10.8
3 b	7.9	8.5	13.1	8.8	8.0	13.3	7.7	7.7	12.0	7.9	7.1	12.5
3 c	70.6	10.8	89.2	12.9	11.5	66.1	71.7	10.3	91.3	11.6	10.1	62.3
only using check points as tie points (no matched tie points)												
2 a	8.6	8.1	10.0	7.9	8.4	10.4	9.6	8.1	9.8	8.0	8.1	11.1
3 a	8.2	8.4	11.2	8.2	8.4	11.2	8.0	8.4	15.4	8.2	9.4	14.7

Table 11: Empirical (ε) rms-values for **set A** and **set B** in [m]

Summarizing it can be stated, that the overall accuracy potential of the combined photogrammetric point determination using selfcalibration methods in this case is approximately 8 m in planimetry and 10 m in height. Regarding the decreased image quality of the HR channel, which adversely affected the point identification, this is a fairly good result. Compared to height accuracies in the order of 5 m, which were reached using MOMS-02/D2 imagery of Australia (Fraser und Shao, 1996), (Baltsavias and Stallmann, 1996), (Kornus, 1997b), the results, however, do not meet the expectations. Considering the relation of the different orbit altitudes, MOMS-2P should result in height accuracies better than 7 m. A possible explanation could be found in the different measurement strategies of the control and check points. Here, the parallaxes between the back and forward looking channels, which mainly infuence the height determination, are a result of point transfer employing the HR-channel. The parallaxes between the back and forward looking channels of the MOMS-02/D2 imagery were directly measured and therefore are supposed to be more accurate.

4 DEM GENERATION

Finally a digital elevation model (DEM) was generated for the entire 3-ray-area, which is approximately covered by the image scenes #28 and #29. Figure 4 shows the major part of the corresponding HR5 image, already superimposed on the generated DEM. The process is subdivided into 4 steps:

1. Derivation of a dense point distribution by least squares matching in image space.
2. Transformation of image points into object space using the interior and exterior orientation of the bundle adjustement.
3. Interpolation of a regular DEM from the resulting object point coordinates, in the following called *MOMS-DEM*.
4. Verification by comparing the MOMS-DEM with reference DEM information.

The DEM quality mainly depends on the accuracy of the mass points but also on the grid size, especially in mountainous areas with higher elevation differences, i.e. a dense network of accurate mass points is required for the production of a precise DEM. Since the matching algorithm, described in section 2.3, did not result in a sufficient number of image points, an alternative least-squares matching algorithm was applied to the imagery of the 3-ray-area. It is a modified region growing algorithm, originally developed by (Otto and Chau, 1989), which already was successfully applied in various line scanner projects (Heipke and Kornus, 1991), (Heipke et al., 1996).

The algorithm starts with at least one pair of homologous points (so-called seed points), which are approximatly known. Normally, image coordinates of GCP are used as seed points, because they have to be measured interactively anyway. Here, the tie points of the first matching run were taken for this purpose. First, a least-squares matching is carried out using the two matrices surrounding the seed points in both images. For the point in the left image remaining unchanged, the exact coordinates of the corresponding point in the right image are computed, as well as the correlation coefficient between the two matrices and other parameters. Next, both matrices are shifted by a constant amount to left (this amount is called *STEP* in the following) and the matching is repeated in the new position. The same is done for the right, on top and under the seed point. The results for all four neighbours of the seed point are entered in a list in the order of decreasing value of the correlation coefficient. The first point of this list is selected as the new seed point. All its remaining neighbours in the distance of STEP are matched and, if the correlation coefficient lies above a certain threshold, the results are entered in the list. If more than one seed point is available, all of them are matched as described and the results are entered in the list. In this way, the whole overlapping area of the two images is processed, producing a regularly spaced grid of points in the left image.

In three runs the image combinations back-fore, back-nadir and fore-nadir were matched using a size of 19 $\times$ 19 pixels for the template matrix and a value of 4 pixels for STEP, corresponding to a distance of 72 m between neighbouring points in object space. The threshold for the correlation coefficient was set to 0.7. From approximately 940.000 possible matches in the 3-ray-area 829.471 corresponding points were found in all three combinations. From the differences of the image coordinates in the nadir channel,

D. Fritsch, M. Englich & M. Sester, eds, 'IAPRS', Vol. 32/4, ISPRS Commission IV Symposium on GIS - Between Visions and Applications, Stuttgart, Germany.

Figure 4: HR5 image of 3-ray-area, perspectively represented using the MOMS-DEM

which were determined twice (combinations back-nadir and fore-nadir), a standard deviation of 0.07 pixel was deduced in x and in y. Thus, 128.804 points showing differences bigger than 0.2 pixels were rejected. Most of these points are located in regions with low image contrast like forest areas, where the accuracy and reliability of the matching process is limited.

The remaining 700.667 image points were transferred into object space by forward intersection using the parameters of the interior and exterior orientation, which were estimated in bundle adjustment run 1a (see section 3.3.2). For each point the three unknown coordinates X, Y and Z were determined in an adjustment, resulting also in residuals for the 6 image coordinates x and y of the three channels. The standard deviations σ_x of the residuals in x were between 0.1 and 0.2 pixels, and σ_y between 0.3 and 0.4 pixels. During the forward intersection further 12.445 points were rejected due to residuals bigger than 3 times σ_x and σ_y, respectively.

For accuracy assessment a DEM of AMilGeo of approximately 5 m accuracy and 25 m grid size was available with reference to the Gauss-Krüger (GK) coordinate system. After transforming the remaining 688.222 points into GK-coordinates the height of the reference DEM H_{ref} was interpolated for the planimetric coordinates of each point and compared to the computed H value H_{MOMS} (also considering a mean local geoidundulation of N=44.7 m). The histogram of the differences ($H_{ref} - H_{MOMS}$) is shown in Figure 5. The statistic analysis leads to the following values:

Minimum difference:	-83.4 m
Maximum difference:	50.9 m
Mean difference:	-2.6 m
Standard deviation:	9.8 m

The analysis using 688.222 points confirms the height accuracy of 9.8 m for the entire 3-ray-area, which already was proved by the

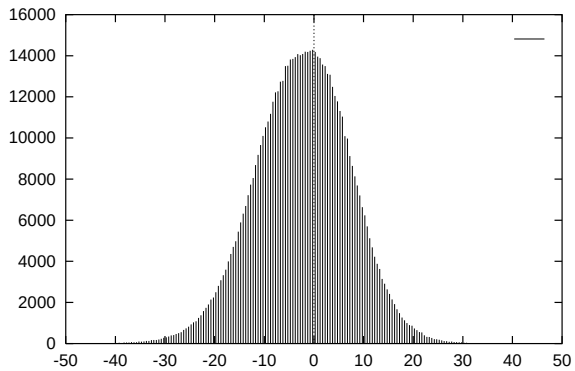

Figure 5: Histogram of differences [m] ($H_{ref} - H_{MOMS}$)

141 check points in version 1a (see Table 11). The mean difference of -2.6 m shows that the reference DEM lies slightly below the MOMS-DEM. This can be explained by the MOMS-DEM representing the visible surface including vegetation and artificial buildings, while the reference DEM solely represents the bare Earth surface. Although many of the points in forest areas already were rejected during the processing (see above), there are still a lot of points left, lying on buildings or tree canopies, causing a difference in the mean height value. The DEM also still contains some single gross errors up to 83 m. The histogram however illustrates, that the differences are normally distributed and no systematic effects are evident, except the already mentioned slight shift of 2.6 m.

Finally a regular DEM with 50 m grid size was calculated by triangular interpolation of the 688.222 object points. By superimposing the image data perspective views can be produced. An example is represented in Figure 4

D. Fritsch, M. Englich & M. Sester, eds, 'IAPRS', Vol. 32/4, ISPRS Commission IV Symposium on GIS - Between Visions and Applications, Stuttgart, Germany.

5 CONCLUSIONS

The presented material documents the results of the digital photogrammetric evaluation of the first threefold along-track stereoscopic MOMS-2P/PRIRODA imagery of Germany, taken from the 390 km high orbit of the MIR space station. Within the 50 km $\times$ 105 km wide area, which is imaged by all 3 viewing directions, an empirical accuracy of 8 m in planimetry and 10 m in height was achieved as verified by 141 independent check points. Additionally a DEM with 50 m grid size of the entire area was generated from 688.222 object points, which previously were derived by least squares image matching and transferred from image to object space using the estimated interior and exterior orientation parameters of the photogrammetric bundle adjustment. A comparison with a 5 m accurate reference DEM (25 m grid size) resulted in a normal distribution of the height differences with a standard deviation of 9.8 m.

In the bundle adjustment the parameters of the interior orientation were simultaneously estimated (selfcalibration), since prior investigations indicated possible deviations of the camera geometry from the laboratory calibration measurements. For 4 parameters siginificant deviations were determined. Furthermore an absolute attitude solution was simultaneously estimated using highly accurate orbit and ground control information. MOMS-2P is operating again since January 1998 and further photogrammetric evaluations using MOMS-2P stereo imagery of other orbits will be performed to verify the results achieved.

6 ACKNOWLEDGEMENT

We would like to thank LTC J. Burkart and W. Quadt from AMilGeo for providing us with the ground control data.

REFERENCES

E. Baltsavias, D. Stallmann: “Geometric Potential of MOMS-02/D2 Data for Point Positioning, DTM and Orthoimage Generation”, *Int. Archives of Photogrammetry and Remote Sensing*, Vol. 31, B4, 110-116, Vienna, Austria, 1996.

B. Eisfeller, S. Föckersperger., A. Jansche, N. Lemke: “MOMSNAV — Location of th Russian Space Station MIR with Differential GPS”, *Kayser-Threde GmbH, Munich*, 1996, paper not published.

S. Föckersperger., R. Hollmann., G. Dick, C. Reigber: “On Board MIR: Orienting Remote Images with MOMSNAV”, *GPS World*, 32-39, October 1997.

C. Fraser, J. Shao: “Exterior Orientation Determination of MOMS-02/D2 Three-Line Imagery: Experiences with the Australian Testfield Data”, *Int. Archives of Photogrammetry and Remote Sensing*, Vol.31, Part B3, 207-214, Vienna, Austria, 1996.

E. Gill: “Orbit determination of the Mir space station from GPS navigation data”, *12th International Symposium on Spaceflight Dynamics*, Darmstadt, 1997.

C. Heipke, W. Kornus: “Nonsemantic photogrammetric processing of digital imagery - the example of SPOT stereo scenes”, *Digital photogrammetric systems*, Ebner H., Fritsch D., Heipke C. (Eds.), 86-102,Wichmann Verlag, Karlsruhe, 1991.

C. Heipke, W. Kornus, A. Pfannenstein: “The evaluation of MEOSS airborne 3-line scanner imagery - processing chain and results”, *Photogrammetric Engineering and Remote Sensing*, Vol.62, No. 3, 293-299, 1996.

O. Hofmann, P. Navé, H. Ebner: “DPS - A digital photogrammetric system for producing digital elevation models and orthophotos by means of linear array scanner imagery”, *Int. Archives of Photogrammetry and Remote Sensing*, Vol. 24-III, 216-227, Helsinki, Finnland, 1982.

W. Kornus, H. Ebner, C. Heipke: “Photogrammetric point determination using MOMS-02/D2 imagery)”, *Proceedings of SPIE Conference on Remote Sensing and Reconstruction for 3-D Objects and Scenes*, 115-125, San Diego, USA, 1995.

W. Kornus, M. Lehner, F. Blechinger, E. Putz: “Geometric Calibration of the Stereoscopic CCD-Linescanner MOMS-2P”, *Int. Archives of Photogrammetry and Remote Sensing, Vol. 31, Part B1*, 90-98, Vienna, Austria, 1996.

W. Kornus: “MOMS-2P Geometric Calibration Report (Version 1.1) - Results of laboratory calibration”, DLR, Institute of Optoelectronics, 1996(a).

W. Kornus: “MOMS-2P: Geometric Calibration (Version 1.2) - Results of band to band registration”, DLR, Institute of Optoelectronics, 1996(b).

W. Kornus: “MOMS-2P Geometric Calibration Report (Version 1.3) - Results of channel 5A/5B registration”, DLR, Institute of Optoelectronics, 1997(a).

W. Kornus: “Dreidimensionale Objektrekonstruktion mit digitalen Dreizeilenscannerdaten des Weltraumprojekts MOMS-02/D2”, Forschungsbericht 97-54 (Dissertation), DLR, Institute of Optoelectronics, 1997(b).

W. Kornus, M. Lehner: “Geometric inflight calibration of the stereoscopic CCD-Linescanner MOMS-2P”, *Proceedings of ISPRS Workshop on ’Sensors and Mapping from Space*, 151-157, Hanover, 1997.

W. Kornus, M. Lehner, M. Schroeder: “Geometric inflight calibration of the stereoscopic CCD-Linescanner MOMS-2P”, *International Archives of Photogrammetry and Remote Sensing, Vol. 32, Part 1*, 148-155, Bangalore, India, 1998.

M. Lehner: “Triple stereoscopic imagery simulation and digital image correlation for MEOSS project”, *International Archives of Photogrammetry and Remote Sensing, Vol. 27, Part 1*, 477-484, Stuttgart, 1986

M. Lehner: “MOMS-2P inflight geometric calibration - measurements for band to band registration based on digital image matching”, DLR, Institute of Optoelectronics, 1996

M. Lehner: “MOMS-2P inflight geometric calibration - measurements for registration of channels 5A/5B based on digital image matching”, DLR, Institute of Optoelectronics, 1997

M. Lehner, R.S. Gill: “Semi-Automatic Derivation of Digital Elevation Models from Stereoscopic 3-Line Scanner Data”, *International Archives of Photogrammetry and Remote Sensing, Vol.XXIX, part B4, Commission IV*, 68-75, Washington, 1992

M. Lehner, W. Kornus: “The photogrammetric evaluation of MOMS-02/D2 mode 3 data (Mexico, Ethiopia)”, *Proceedings of International Workshop on International Mapping from Space Nov.27-Dec.1 1995*, 51-68, Madras, India, 1996.

M. Lehner, W. Kornus: “Band to Band Registration of MOMS-2P Camera”, *Proceedings of ISPRS Workshop on ’Sensors and Mapping from Space*, 155-162, Hanover, 1997.

G. Otto, T. Chau: “Region growing algorithm for matching of terrain images”, *Image and vision computing*, (7) 2, 83-94, 1989.

P. Seige, P. Reinartz, M. Schroeder: “The MOMS-2P mission on the MIR station”, *International Archives of Photogrammetry and Remote Sensing, Vol. 32, Part 1*, Bangalore, India, 1998.